

# In-beam fast-timing measurements in $^{103,105,107}\text{Cd}$

S. Kisiov<sup>1</sup>, S. Lalkovski<sup>1\*</sup>, N. Mărginean<sup>2</sup>, D. Bucurescu<sup>2</sup>, L. Atanasova<sup>3</sup>, D. L. Balabanski<sup>3</sup>, Gh. Căta-Danil<sup>2</sup>, I. Căta-Danil<sup>2</sup>, J.-M. Daugas<sup>4</sup>, D. Deleanu<sup>2</sup>, P. Detistov<sup>3</sup>, D. Filipescu<sup>2</sup>, G. Georgiev<sup>5</sup>, D. Ghiță<sup>2</sup>, T. Glodariu<sup>2</sup>, J. Jolie<sup>6</sup>, D.S. Judson<sup>7</sup>, R. Lozeva<sup>5</sup>, R. Mărginean<sup>2</sup>, C. Mihai<sup>2</sup>, A. Negret<sup>2</sup>, S. Pascu<sup>2</sup>, D. Radulov<sup>1†</sup>, J.-M. Régis<sup>6</sup>, M. Rudigier<sup>6</sup>, T. Sava<sup>2</sup>, L. Stroe<sup>2</sup>, G. Suliman<sup>2</sup>, N.V. Zamfir<sup>2</sup>, K.O. Zell<sup>6</sup> and M. Zhekova<sup>1</sup>

<sup>1</sup>*Faculty of Physics, University of Sofia "St. Kliment Ohridski",  
1164 Sofia, Bulgaria;*

<sup>2</sup>*Horia Hulubei National Institute for Physics and Nuclear Engineering,  
77125 Bucharest-Magurele, Romania*

<sup>3</sup>*Institute for Nuclear Research and Nuclear Energy,  
Bulgarian Academy of Science, 1784 Sofia, Bulgaria*

<sup>4</sup>*CEA, DAM, DIF, 91297 Arpajon, France*

<sup>5</sup>*Centre de Spectrométrie Nucléaire et Spectrométrie de Masse,  
91405 Orsay-Campus, France*

<sup>6</sup>*Institut für Kernphysik,*

*University of Cologne, Cologne, Germany*

<sup>7</sup>*Department of Physics, University of Liverpool,  
Liverpool, United Kingdom*

(Dated: January 20, 2013)

Fast-timing measurements were performed recently in the region of the medium-mass  $^{103,105,107}\text{Cd}$  isotopes, produced in fusion evaporation reactions. Emitted  $\gamma$ -rays were detected by eight HPGe and five  $\text{LaBr}_3\text{:Ce}$  detectors working in coincidence. Results on new and re-evaluated half-lives are discussed within a systematic of transition rates. The  $7/2_1^+$  states in  $^{103,105,107}\text{Cd}$  are interpreted as arising from a single-particle excitation. The half-life analysis of the  $11/2_1^-$  states in  $^{103,105,107}\text{Cd}$  shows no change in the single-particle transition strength as a function of the neutron number.

PACS numbers: 21.10.k, 21.10.Hw, 21.10.Tg, 23.20.Lv, 27.60.+j

## I. INTRODUCTION

Cadmium isotopes have two protons less than the  $_{50}\text{Sn}$  nuclei, presenting a good test case for the robustness of the shell structure. Shell model calculations successfully describe the experimentally observed level energies and level lifetimes in the extreme neutron-rich and neutron-deficient cadmium isotopes proving the persistence of the shell structure below the doubly magic  $^{132}\text{Sn}$  and  $^{100}\text{Sn}$  [1–4]. Fingerprints of collectivity, however, start to emerge when moving away from the neutron shell closures. They can be found in the decrease of the  $2_1^+$  energy and in the increase of the respective  $B(E2; 2_1^+ \rightarrow 0_1^+)$  values when approaching the neutron mid-shell [5].

Due to the neighbourhood of the shell model tin isotopes and the presence of weak collectivity in the neutron-mid shell cadmium isotopes, both single particle and collective states are expected to occur in the medium mass odd-A Cd nuclei. Moreover, there are several cases where the structure of the state is ambiguous. In the  $^{103,105,107}\text{Cd}$  [6–8], for example, the lowest-lying excited  $J^\pi = 7/2^+$  state can arise from a collective excitation built on the  $5/2^+$  ground state or from a single-particle excitation. A model independent approach to the prob-

lem is to evaluate the  $B(E2)$  transition strengths within a systematical study involving even-even well deformed and spherical nuclei, where the structure is well established.

In order to study the structure of the low-lying excited states in  $^{103,105,107}\text{Cd}$  fast-timing measurements were performed. The half-lives are directly related to the transitions rates and hence to the structure of the state. The present paper reports on new results, obtained with eight HPGe detectors working in coincidence with five  $\text{LaBr}_3\text{:Ce}$  detectors.

## II. EXPERIMENTAL SET UP

The low-lying excited states, placed on and close to the yrast line in  $^{103}\text{Cd}$ ,  $^{105}\text{Cd}$  and  $^{107}\text{Cd}$  were populated via fusion evaporation reactions. A carbon beam, accelerated to 50 MeV by the Tandem accelerator of the National Institute for Physics and Nuclear Engineering at Magurele, Romania, impinged on self-supporting 10 mg/cm<sup>2</sup> thick  $^{94,96}\text{Mo}$  targets and on a 1 mg/cm<sup>2</sup> thick  $^{98}\text{Mo}$  target with 20  $\mu\text{m}$  Pb backing. The three targets were isotopically enriched up to 98.97% in  $^{94}\text{Mo}$ , 95.70% in  $^{96}\text{Mo}$  and 98% in  $^{98}\text{Mo}$ , respectively.

The cross section for the  $^{94}\text{Mo}(^{12}\text{C}, 3n)^{103}\text{Cd}$  reaction was calculated to be 100 mb, while for the  $^{96}\text{Mo}(^{12}\text{C}, 3n)^{105}\text{Cd}$  and  $^{98}\text{Mo}(^{12}\text{C}, 3n)^{107}\text{Cd}$  reactions it was approximately 400 mb. The typical beam intensity

\*E-mail address: stl@phys.uni-sofia.bg

†Present address: Katholieke Universiteit, Leuven, Belgium

was of the order of 8 pnA. Besides the 3n channels, the 4n, 2np, 4np and 2n $\alpha$ - fusion evaporation channels also have significant cross sections which contaminate the spectra of interest.

The half-lives of the levels of interest were deduced by using a fast-timing set up consisting of 5 LaBr<sub>3</sub>:Ce scintillator detectors working in coincidences with 8 HPGe detectors [9]. Five of the HPGe detectors were placed at backward angles with respect to the beam axis, two were placed at 90° and the eighth HPGe detector was placed at a forward angle. The five LaBr<sub>3</sub>:Ce detectors were mounted bellow the target chamber on a ring of approximately 45° degrees with respect to the beam axis. The five LaBr<sub>3</sub>:Ce crystals had a cylindrical shape and 5% Ce doping. One of the LaBr<sub>3</sub>:Ce detector was a commercial integral detector. Its size was 2"×2". Two of the LaBr<sub>3</sub>:Ce detectors had 1" height and a diameter of 1". Two LaBr<sub>3</sub>:Ce crystals had dimensions of 1.5"×1.5". Each of the four crystals was optically coupled to XP20D0B photomultiplier and mounted in aluminum casing. The readout, from each of the four non-commercial detectors, was made via a VD184/T voltage divider. The voltage divider issues a negative anode signal and a fast positive dynode signal. The anode signal was used for timing, while the dynode signal was used to obtain energy signal. This non conventional choice was made to avoid the saturation of the dynode signal [9], which facilitates the analysis of the energy spectra.

The energy signals from the HPGe detectors were amplified and then digitized by 8k Analog to Digital Converters (ADC) AD413A. The timing signals from the HPGe detectors were processed by 4k 4418/T Time-to-Digital converters. The energy signals from the LaBr<sub>3</sub>:Ce detectors were amplified by spectroscopic amplifiers and then digitized by 8k ADC AD413A. The timing signals from the LaBr<sub>3</sub>:Ce detectors were sent to a Quad Constant Fraction Discriminator, model 935. Each of the five timing signals was used to start a Time-to-Amplitude Converter (TAC) operating in a common stop mode. Then the five TAC output signals were sent to 8k ADCs. The acquisition was triggered when two LaBr<sub>3</sub>:Ce and one HPGe detectors were fired in coincidences.

### III. DATA ANALYSIS

Data was stored in event-by-event mode in 100 MB long files, which were grouped in runs of approximately 2 hours. Then the data was analyzed using the GASPWare and Radware [10] packages. Because of the instability of the LaBr<sub>3</sub>:Ce detectors observed with time, a gain matching procedure was applied run-by-run. To correct the CFD for the walk effect, observed at low energies, analysis of the time response as a function of energy was performed with a <sup>60</sup>Co source [9] and in-beam. Then the data was sorted in gated energy spectra, two-dimentional energy-energy ( $E_\gamma - E_\gamma$ ) and three-dimentional energy-energy-time ( $E_\gamma - E_\gamma - \Delta T$ ) matrices, where  $E_\gamma$  is the

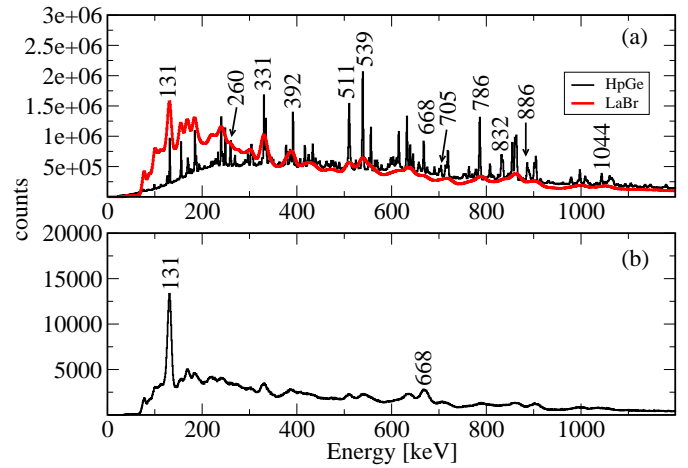


FIG. 1: (Colour online) <sup>105</sup>Cd energy spectra: (a) Total projection from all HPGe and LaBr<sub>3</sub>:Ce detectors; (b) LaBr<sub>3</sub>:Ce energy spectrum gated on a 886-keV transition in any of the HPGe detectors. The labels denote transitions in <sup>105</sup>Cd

$\gamma$ -ray energy detected by a LaBr<sub>3</sub>:Ce detector and  $\Delta T$  is a time difference between two gamma rays detected in coincidence.

The ( $E_\gamma - E_\gamma - \Delta T$ ) matrices were constructed as fully symmetric in energy, i.e. for each event where  $\gamma$ -rays of energies  $E_{\gamma 1}$  and  $E_{\gamma 2}$  are detected the matrix elements ( $E_{\gamma 1}, E_{\gamma 2}$ ) and ( $E_{\gamma 2}, E_{\gamma 1}$ ) are incremented, while the time intervals associated with these two points are calculated as  $\Delta T = (t_1 - t_2) + t_0$  and  $\Delta T = -(t_1 - t_2) + t_0$  respectively. Here,  $t_1 - t_2 > 0$  is the time difference measured with two TAC converters and  $t_0$  is an arbitrary offset. In the cases where the two  $\gamma$ -rays feed and de-excite a state with a half-life longer than the electronics resolution, which in the present work is 6 ps/channel, then the time distributions associated with the two matrix elements ( $E_{\gamma 1}, E_{\gamma 2}$ ) and ( $E_{\gamma 2}, E_{\gamma 1}$ ) will be shifted by  $2\tau$ , where  $\tau$  is the lifetime of the level of interest. This procedure represents the centroid shift method [11], which has been successfully used in the past [12] and recently applied with LaBr<sub>3</sub>:Ce detectors [9]. In the cases, where the level half-life is much longer than the detector time resolution, a tail emerges on the right hand side of the time distribution. In these cases the slope of the tail has been used to determine the half-life of the level. Deconvolution of Gaussian and exponent was applied in the cases where the half-life of the level is of the order of the FWHM of the prompt distribution.

In order to select a particular reaction channel and particular  $\gamma$ -decay branch leading to the state of interest, the matrices were constructed with a condition imposed on prompt  $\gamma$ -rays detected in any of the high-resolution HPGe detectors.

Fig. 1(a) shows the energy total projection for the <sup>12</sup>C+<sup>96</sup>Mo→<sup>105</sup>Cd+3n reaction for all HPGe and LaBr<sub>3</sub>:Ce detectors. At low energies, the higher efficiency of the LaBr<sub>3</sub>:Ce with respect to the HPGe detectors is remarkable. The energies of <sup>105</sup>Cd are marked

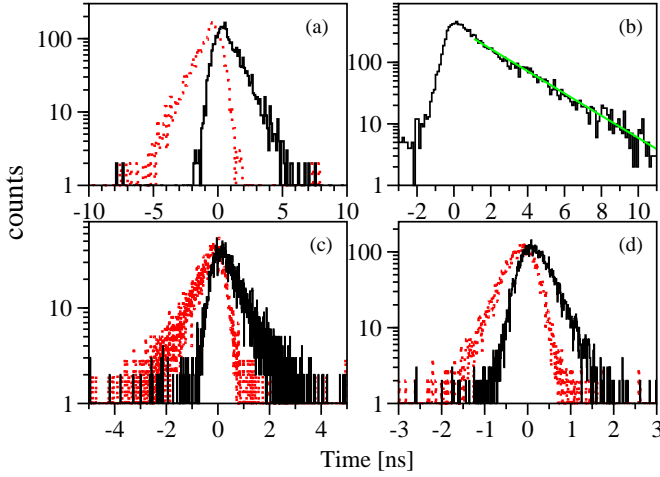


FIG. 2: (Colour online) Time spectra, obtained for the decay of the  $7/2_1^+$  states in  $^{107}\text{Cd}$  (a),  $^{105}\text{Cd}$  (b),  $^{103}\text{Cd}$  (c) and for the  $11/2_1^-$  state in  $^{105}\text{Cd}$  (d)

with numbers. Fig. 1(b) represents the LaBr<sub>3</sub>:Ce energy spectrum, gated on the 886-keV transition from  $^{105}\text{Cd}$  in the HPGe detectors, which improves the peak-to-background ratio. Similar spectra were constructed for the other two reactions  $^{12}\text{C}+^{94}\text{Mo}\rightarrow^{103}\text{Cd}+3n$  and  $^{12}\text{C}+^{98}\text{Mo}\rightarrow^{107}\text{Cd}+3n$ .

Fig. 2 presents time spectra obtained after two dimensional energy gates imposed on  $E_\gamma-E_\gamma - \Delta T$  matrices, gated on prompt transitions with HPGe detectors. To increase the statistics, in each of the cases, several prompt gates were imposed on the HPGe detectors. Here, the procedure will be illustrated by using the lowest lying prompt and delayed transitions shown on Fig. 3.

Fig. 2(a) presents the time distributions for the decay of the  $7/2_1^+$  state in  $^{107}\text{Cd}$ . The time distribution, plotted in full lines, is obtained with a (205 $\gamma$ , 641 $\gamma$ ) energy gate, while the symmetric (641 $\gamma$ , 205 $\gamma$ ) gate is plotted with dots. The half-life of 0.68 (4) ns, obtained from the centroid shift method, is consistent with the NNDC value of  $T_{1/2}=0.71$  (4) ns [8]. Gates on 798-keV or 956-keV transitions (Fig. 3) were applied with HPGe detectors in order to clean the time spectra from background events.

Fig. 2(b) presents the time curves for the decay of the  $7/2_1^+$  state in  $^{105}\text{Cd}$ . The half-life of 1.66 (12) ns, obtained in the present study, was measured from the slope of the time distribution gated on (639 $\gamma$ -131 $\gamma$ ) with the LaBr<sub>3</sub>:Ce detectors and cleaned with a gate on the 886  $\gamma$ -ray or 705-keV  $\gamma$ -ray (Fig. 3) imposed on any of the eight HPGe detectors. It agrees the 1.75 (11) ns value, adopted by NNDC [7], which is based on a  $\gamma(t)$  measurement with one NaI(Tl) detector [13].

Fig. 2(c) presents the time curves for the decay of the  $7/2_1^+$  state in  $^{103}\text{Cd}$ . The half-life of 0.37 (3) ns was obtained from the centroid shift of the two time distributions generated with gates on the 188-keV and 720-keV transitions (Fig. 3) imposed on any two of the LaBr<sub>3</sub>:Ce detectors in coincidence with the 921-keV or 623-keV  $\gamma$ -

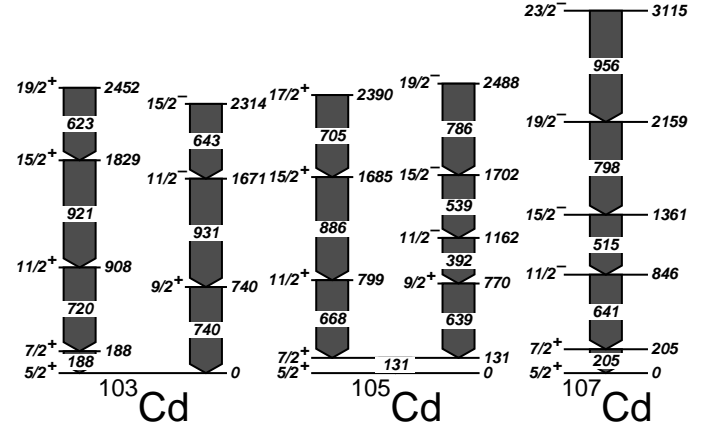


FIG. 3: Partial level schemes of  $^{103,105,107}\text{Cd}$

TABLE I: First excited  $7/2^+$  state in  $^{103,105,107}\text{Cd}$  and decay properties

Isotope	$E_i$ [keV]	$T_{1/2}$	$E_\gamma$ [keV]	$L\lambda$	$\delta$	$B(\lambda L)$ [W.u.]
$^{103}\text{Cd}$	188	0.37 (3) ns	188	M1	$\leq 0.1$	0.0089 (8)
				E2		2.27 (19)
$^{105}\text{Cd}$	131	1.66 (12) ns	131	M1	$\leq 0.1$	0.0058 (5)
				E2		2.93 (22)
$^{107}\text{Cd}$	205	0.68 (4) ns	205	M1	0.25 (1)	0.00331 (20)
				E2		4.2 (4)

rays (Fig. 3) detected in any of the HPGe detectors.

The half-life of the  $11/2_1^-$  state in  $^{105}\text{Cd}$  Fig. 2(d) was obtained by gating on the 539-keV feeding and 392-keV de-exciting transitions (Fig. 3), detected by any two of the five LaBr<sub>3</sub>:Ce detectors. An additional gate on the 786-keV  $\gamma$ -ray, which is in coincidence with the 392-keV and 786-keV transitions (Fig. 3), was imposed on any of the HPGe detectors. The half-life, deduced from the centroid shift of the two mirror time spectra, is 149 (12) ps.

#### IV. DISCUSSION

**$7/2_1^+$** : The half-lives  $T_{1/2}$ , of the levels of interest, are listed in Table I along with the level energy  $E_i$  and the spin/parity assignments  $J^\pi$ . In order to calculate the partial half-lives and the reduced transition probabilities the  $\gamma$ -ray energies  $E_\gamma$ , multipolarities  $L\lambda$ , and mixing ratios  $\delta$ , adopted by NNDC [6–8], are also listed. The  $J^\pi = 7/2^+$  state is the first excited state in all three isotopes and decays via M1+E2 transition to the ground state. An upper limit of the mixing ratio  $\delta \leq 0.1$  for the  $7/2_1^+ \rightarrow 5/2_1^+$  transition in  $^{103}\text{Cd}$  has been estimated by the NNDC [6]. The mixing ratio, adopted for the M1+E2 transition in  $^{107}\text{Cd}$ , is  $\delta = +0.25$  (1) [8]. It has been suggested that the respective transition in  $^{105}\text{Cd}$  is of almost pure M1 nature, however a small E2 admixture

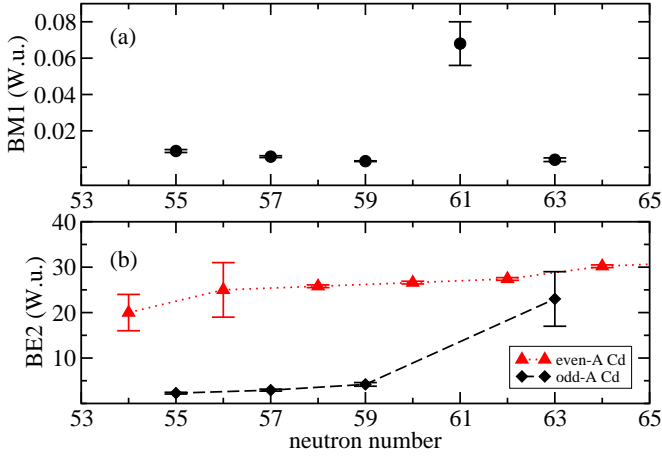


FIG. 4: (Colour online) Systematics of (a)  $B(M1; 7/2_1^+ \rightarrow 5/2_1^+)$  values for odd-A cadmium nuclei and (b)  $B(E2; 7/2_1^+ \rightarrow 5/2_1^+)$  values for odd-A cadmium isotopes (diamonds) compared to the  $B(E2; 2_1^+ \rightarrow 0_1^+)$  values in even-even cadmium cores (triangles)

is assumed [7]. For the purpose of the current discussion an upper limit of  $\delta \leq 0.1$  was adopted in the present study.

The reduced transition probabilities, calculated with RULER [5], are given in the last column of Table I.

Fig. 4 shows the systematic trend of the  $B(M1)$  (Fig. 4(a)) and  $B(E2)$  values for the  $7/2_1^+ \rightarrow 5/2_1^+$  transitions in  $^{103-111}\text{Cd}_{55-63}$  (Fig. 4(b)), compared to the  $B(E2; 2_1^+ \rightarrow 0_1^+)$  for their even-even Cd cores. Fig. 5 shows the evolution of the  $B(E2; 2_1^+ \rightarrow 0_1^+)$  transition rates with the neutron number for all even-even nuclei in the  $40 \leq Z \leq 50$  region.

In the  $^{103-107}\text{Cd}_{55-59}$  nuclei, because of the low mixing ratio, the  $B(E2; 7/2_1^+ \rightarrow 5/2_1^+)$  transition strenghts are significantly suppressed in comparison to the  $B(E2; 2_1^+ \rightarrow 0_1^+)$  values for the even-even Cd cores (Fig. 4(b)). Moreover, they are two orders of magnitude weaker than the  $B(E2; 2_1^+ \rightarrow 0_1^+)$  values for the most deformed neutron mid-shell Zr and Mo nuclei (Fig. 5). In fact, the  $^{103,105,107}\text{Cd}$   $B(E2; 7/2_1^+ \rightarrow 5/2_1^+)$  values are similar to the reduced transition probabilities for the magic tin nuclei (Fig. 5) suggesting a single-particle nature of the  $7/2_1^+$  state, most probably arising from  $\nu g_{7/2}$  configuration.

In  $^{109}\text{Cd}_{61}$ , the  $7/2_1^+$  state appears 203 keV above the  $5/2_1^+$  ground state and decays via a pure, according to NNDC, M1 transition giving rise to  $B(M1)(\text{W.u.}) = 0.068$  [14], which is an order of magnitude higher than the respective value in  $^{103-107}\text{Cd}$ . However, the odd behavior of the  $B(M1)$  point on Fig. 4 suggests a significant E2 component. In fact, such an increase of the  $B(E2)$  value, and hence in the collectivity of the state, is observed in  $^{111}\text{Cd}$ . There, the  $5/2_1^+$  and  $7/2_1^+$  states appear at 245 keV and 416 keV respectively [15]. The  $7/2_1^+$  has a half-life of 0.12 ns and decays to the  $5/2_1^+$  state via 171-keV M1+E2 transition. The mixing ratio  $\delta = -0.144$  of this transition leads to  $B(E2; 7/2_1^+ \rightarrow 5/2_1^+) = 23.6(2)$  W.u.,

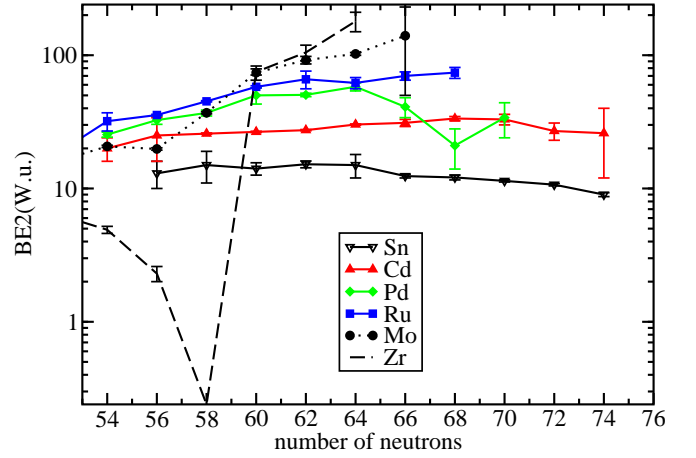


FIG. 5: (Colour online) Systematics of  $B(E2; 2_1^+ \rightarrow 0_1^+)$  transition rates for the even-even nuclei with  $40 \leq Z \leq 50$

which approaches the  $B(E2; 2_1^+ \rightarrow 0_1^+)$  value in the even-even cadmium cores (Fig. 4(b)) and hence the  $7/2_1^+$  state becomes collective.

**$11/2_1^-$ :** The  $J^\pi = 11/2_1^-$  states appear in all odd-cadmium isotopes from  $^{103}\text{Cd}$  to  $^{123}\text{Cd}$  [5]. It is observed at 1671 keV in  $^{103}\text{Cd}$  [6] and decreases in energy when approaching the neutron mid-shell. In  $^{117}\text{Cd}_{69}$  it appears at 136 keV above the ground state.

The big energy gap between the  $11/2_1^-$  state and the ground state in  $^{103-111}\text{Cd}$  opens space for several states of single-particle and collective nature to appear. Among those levels is the  $9/2_1^+$  state to which the  $11/2_1^-$  state decays via an E1 transition. For medium mass odd-A Cd isotopes the energy of the  $11/2_1^-$  drops closer to the ground state where only low-spin states are populated. In this mass region the  $11/2_1^-$  state decays via low-energy transitions of higher multipolarity leading to increase of its half-life to  $T_{1/2} = 14.1$  y in  $^{113}\text{Cd}$  [5]. Further increases of the energy of the  $11/2_1^-$  state with respect to the ground state leads to a decrease of the half-life. The isomeric  $11/2_1^-$  state in all neutron-rich cadmium nuclei with  $A \geq 113$  decay via  $\beta$ -decay process to the respective indium isobars. In spite the half-life of the state decreases and the energy of the isomeric state increases with the mass number, isomeric decays have not been observed so far.

The half-life of the excited  $11/2_1^-$  state in  $^{103,105}\text{Cd}$ , measured in present work, allows a systematical study of the E1 transitions strenghts as a function of the neutron number. The half-life  $T_{1/2} = 71$  ns of the  $11/2_1^-$  state in  $^{107}\text{Cd}$  has been previously measured [13]. This level decays via a branch of E1, M2 and E3 transitions to  $9/2_1^+$ ,  $7/2_1^+$  and  $5/2_1^+$  states with partial half-lives  $2.4 \times 10^{-7}$ ,  $1.0 \times 10^{-7}$  and  $4.5 \times 10^{-6}$  s respectively.

The  $11/2_1^-$  state in  $^{105}\text{Cd}$ , which has a  $T_{1/2} = 149$  ps, decays via two E1 transitions to two  $9/2_1^+$  states. The partial half-lives for the two transitions are  $2.7 \times 10^{-10}$  and  $3.3 \times 10^{-10}$  s respectively.

The  $11/2_1^-$  state in  $^{103}\text{Cd}$  decays via a 931-keV E1

transition to a  $9/2^+$ . No time structure of the decaying transition was observed in the present work. Therefore, an upper limit of 6 ps was deduced.

The Weisskopf estimates for the 931-keV E1  $\gamma$ -ray in  $^{103}\text{Cd}$  is  $T_{1/2}^{W.e.} = 3.8 \times 10^{-16}$  s, for the 330-keV E1 transition and 392-keV E1  $\gamma$ -ray in  $^{105}\text{Cd}$  are  $8.40 \times 10^{-15}$  s and  $5.00 \times 10^{-15}$  s. and  $T_{1/2}^{W.e.} = 6.14 \times 10^{-12}$  s for the 37-keV E1 transition in  $^{107}\text{Cd}$ . For all four transitions the E1 hindrance factor  $F^W = T_{1/2,\gamma}/T_{1/2}^{W.e.}$  is of order of  $10^4$ . Given that the  $11/2^-$  is an intruder state, the similar hindrance factor observed in all three odd-A cadmium nuclei  $^{103,105,107}\text{Cd}$  suggests similar structure of the final  $9/2^+$  state.

## V. CONCLUSION

Excited states in  $^{103,105,107}\text{Cd}$  have been populated via fusion-evaporation reactions. Half-lives of several excited states were measured by using the delayed coincidence

technique. The half-life of the  $7/2_1^+$  state in  $^{107}\text{Cd}$  and  $^{105}\text{Cd}$  were confirmed. The half-life of the first excited state in  $^{103}\text{Cd}$  and of the  $11/2_1^-$  in  $^{105}\text{Cd}$  are newly obtained allowing a systematical study of the transitions strenghts. The  $B(E2; 7/2_1^+ \rightarrow 5/2_1^+)$  transitions strenghts in  $^{103-107}\text{Cd}$  are strongly hindered with respect to the  $B(E2; 2_1^+ \rightarrow 0_1^+)$  values, observed in the most deformed nuclei in the region, suggesting a single particle nature for the  $7/2_1^+$  states. The hindrance factors, calculated for E1 transitions in  $^{103,105,107}\text{Cd}$ , suggest similar structure of the  $9/2^+$  states.

## VI. ACKNOWLEDGMENTS

The work is partly supported by the Bulgarian Science Fund under contracts DMU02/1, DRNF02/5, DID-05/16 and by a contract for Bularian-Romanian partnership, number BRS-07/23.

- 
- [1] A. Jungclaus *et al.*, Phys. Rev. Lett. **99**, 132501 (2007)
  - [2] L. Caceres *et al.*, Phys. Rev. C **79**, 011301 (2009)
  - [3] F. Naqvi *et al.*, Phys. Rev. C **82**, 034323 (2010)
  - [4] A. Blazhev *et al.*, Phys. Rev. C **69**, 064304 (2004)
  - [5] NNDC data base (www.nndc.bnl.gov)
  - [6] D. de Frenne, Nucl. Data Sheets **110**, 2081 (2009)
  - [7] D. de Frenne and E. Jacobs, Nucl. Data Sheets **105**, 775 (2005)
  - [8] J. Blachot, Nucl. Data Sheets **109**, 1383 (2008)
  - [9] N. Mărginean *et al.*, Eur. Phys. J. **A46**, 329 (2010)
  - [10] D. Radford, Nucl. Instr. Meth. **A361**, 297 (1995)
  - [11] W. Andrejtscheff, M. Senba, N. Tsoupas and Z. Z. Ding, Nucl. Instr. Meth. **204**, 123 (1982)
  - [12] W. Andrejtscheff, L. K. Kostov, H. Rotter, H. Prade, F. Sary, M. Senba, N. Tsoupas, Z. Z. Ding and P. Raghavan, Nucl. Phys. **A437**, 167 (1985)
  - [13] R. Rougny, M. Meyer-Lévy, R. Béraud, J. Rivier and R. Moret, Phys. Rev. C **8**, 2332 (1973)
  - [14] J. Blachot, Nucl. Data Sheets **107**, 355 (2006)
  - [15] J. Blachot, Nucl. Data Sheets **110**, 1239 (2009)